Photon Factory Activity Report 2001 #19B
–Users' Report–

16B/1999G007

Measurement of two-photon correlation of synchrotron radiation by delay modulation technique

Yasuhiro TAKAYAMA*[1], Chol LEE[1], Kenji OBU[1], Hidetsugu SHIOZAWA[1], Tsuneaki MIYAHARA[1], Shigeru YAMAMOTO[2], Masami ANDO[2]
[1]Tokyo Metropolitan Univ., 1-1, Minamiohsawa, Hachioji-shi, Tokyo 192-0397, Japan
[2]KEK-PF, Tsukuba, Ibaraki, 305-0801, Japan

Introduction

Two-photon correlation (second order coherence) has been measured in order to investigate the photon statistics and spatial coherence of synchrotron radiation. However, the signal corresponding to the two photon correlation was extremely small due to the short coherent time compared with the response time of the detector or electric circuit. To overcome the difficulty, Tai et al. have developed a new idea to modulate the coherence time and measured the signal with a lockin amplifier. They have succeeded in observing a bunching effect originated from the chaotic nature of the synchrotron radiation [1][2]. In this study, we adopted another technique to modulate the delay time and measured the signal by a lockin amplifier. By this technique, the bunching effect was more clearly observed [3].

Experimental

The experiment was performed at an undulator beamline BL-16B. The monochromatized beam with the photon energy of 60 eV was diffracted by a Fraunhofer slit and the spatial coherence was controlled by the slit. The beam was divided into two pieces and each beam was measured by a photomultiplier tube (PMT). The separation between the time that a photon arrived to a PMT and the time that another photon arrived to the other PMT was measured by a set of modules composed of a constant fraction discriminator (CFD), a time to amplitude converter (TAC) and two solid state switches. There are two paths with different delays between the CFD and the stop input of the TAC, and the solid state switches can control which path the signal goes through. Output of the TAC came into a single channel analyzer (SCA) and the pulse with the selected height was discriminated. The SCA was adjusted so that the signal from the SCA appeared only when two photons were simultaneously detected by each PMT, respectively. The output of the SCA came into a ratemeter and the analog output of the ratemater was measured by a digital lockin amplifier. We switched the paths between the CDF and stop input of the TAC by a function generator with the frequency of 0.49999 Hz, which was also used as a reference input of the lockin amplifier. The x component of the lockin amplifier $-V_x$ has the information on the second order coherence. We accumulated the data for about 4 hours for several width of the Fraunhofer slit D.

Result and discussions

Figure 1 shows the plot of $-V_x$ as a function of the width of the Fraunhofer slit D. As D is smaller, the correlation of the light at the two PMTs becomes stronger. Hence, $-V_x$, which is proportional to the integral of the second order coherence on the Fraunhofer slit, increases. This phenomena is known as the bunching effect of the chaotic light. The experiment clearly shows that the synchrotron radiation of the PF in VUV region has a chaotic component. If the light is chaotic, the first order coherence can be known from the second order coherence. Since the electron-beam emittance can be estimated from the first order coherence, we can estimate the electron-beam emittance from this experiment with the knowledge of the beamsize on the Fraunhofer slit. The beamsize measured with a tungsten wire scanner was 507 μm and the electron-beam emittance was estimated as 135 nmrad, which was much larger than the designed value of 36 nmrad. The reason of the discrepancy may be a rough approximation to derive a theoretical prediction.

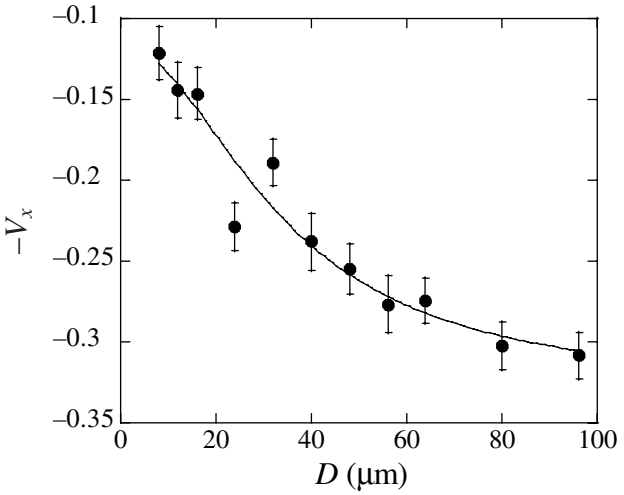

Figure 1: Output of the lockin amplifier as a function of the width of Fraunhofer slit.

References

[1] R. Z. Tai et al., Phys. Rev. A. **60**, 3262 (2000).
[2] H. Shiozawa et al., PF Activity Report 19B, 277(2001).
[3] Y. Takayama et al., J. Synchrotron. Rad. (2002). submitted.

* takayama@phys.metro-u.ac.jp

8C/1999S2-003

Development of X-ray depolarizer based on phase retarder – Generation of depolarized X-rays from polarized X-rays –

Yoshinori UEJI [1] , Kohei OKITSU[2], and Yoshiyuki AMEMIYA*[1, 3]
[1]Department of Applied Physics, Univ. of Tokyo, Bunkyo-ku, Tokyo 113-8656 Japan
[2]Engineering Research Institute, Univ. of Tokyo, Bunkyo-ku, Tokyo 113-8656 Japan

Introduction

Recently polarization property of synchrotron radiation has been utilized in some experiments such as X-ray magnetic circular dichroism and ATS scattering. Incidentally most of samples of interest are more or less sensitive to X-ray polarization. Therefore, strictly speaking, it is necessary to characterize the polarization of incident X-ray beam to a sample regardless of the intention whether or not to utilize the polarization property, though it is not practical. It is also not easy to calculate the polarization of incident X-ray beam, because the polarization property depends on optical elements such as mirrors and monochromator. Therefore, it would be beneficial to utilize non-polarized X-ray in stead of not-well-defined polarized X-ray for the experiments in which the use of polarized X-rays is not intended and/or complicates the data analysis. For an example, multi-wavelength anomalous dispersion (MAD) method widely used in protein structure analysis assumes no polarization dependence of anomalous scattering factors. Here, we will propose an idea to use a transmission-type X-ray phase retarder [1] as a depolarizer in order to generate non-polarized X-ray from the polarized synchrotron X-ray radiation.

An X-ray phase retarder is an optical component to utilize double refraction taking place in the vicinity of Bragg condition in perfect crystals like silicon and diamond. The phase shift between σ- and π- component is approximately proportional to the inverse of deviation angle from Bragg condition. Therefore, it rapidly changes at the most vicinity of Bragg condition, whereas it slowly changes in a region further from Bragg condition where it is usually used as phase retarder. If the phase retarder is set just at Bragg condition, random phase shift is given to the incident beam on average and results in generating pseudo non-polarized X-ray whose polarization states are uniformly distributed along a great circle which passes through the north and south pole on the Poincaré sphere. We will report on the performance of a pseudo depolarizer based on a phase retarder.

Experimental

The depolarizer has been evaluated by using a sample which shows linear dichroism (LD). We have compared the magnitude of LD with two different incident beams: one with (a) only polarizer and the other with (b) polarizer+depolarizer (Fig.1).

The energy of the incident X-ray is set at the cobalt *K* absorption edge (7709 eV). The energy spread is about 1 eV, and the horizontal beam divergence is 20 arcsec. The phase retarder is a (100)-oriented diamond (about 300 m thickness) crystal giving 111 reflection in an asymmetric Laue geometry. The sample used is an *h.c.p.* cobalt single crystal.

Results and Discussion

The absorption coefficient (μt) of (b) was normalized to that of (a) at the absorption edge. The magnitude of linear polarization has been decreased to less than 5% by the use of the depolarizer (Fig. 1). It means that the degree of the linear polarization is decreased to 5%. The loss of the X-ray intensity with the depolarizer is 50%. The obtained non-polarized X-ray beam will be useful to XAFS, MAD experiment for protein crystallography.

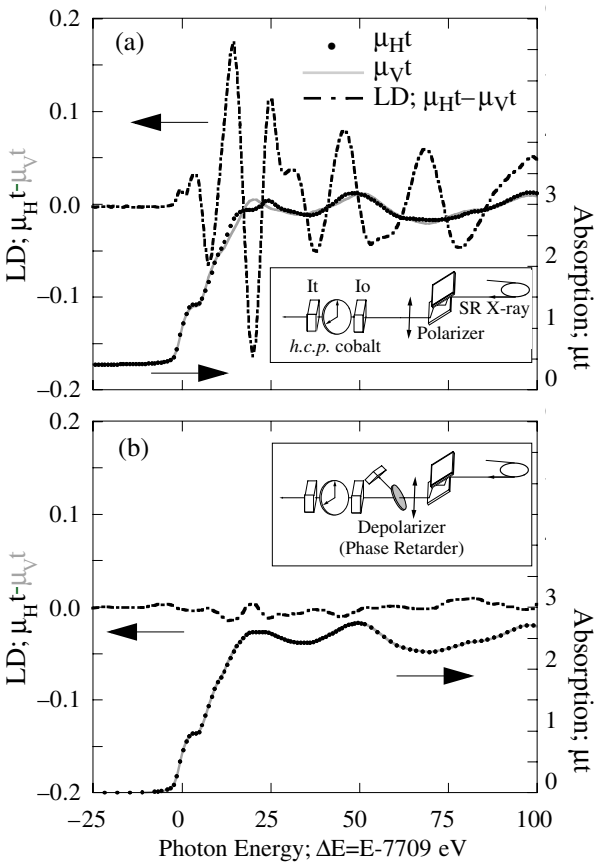

Figure 1: Evaluation of the depolarizer

References

[1] K. Hirano, T. Ishikawa, and S. Kikuta: Rev. Sci. Instrum. **66** (1995) 1604.

Present address: Department of Advanced Materials Science, Univ. of Tokyo, Kashiwa, Chiba 277-8581, Japan

* amemiya@k.t.u-tokyo.ac.jp

8C$_2$/1999S2-003

Generation of arbitrary X-ray polarization by rotatable four-quadrant diamond phase-retarder system

Yuta URANO[1], Yoshinori UEJI[1], Kouhei OKITSU[2], Yoshiyuki AMEMIYA[1]
[1]Department of Applied Physics, The University of Tokyo, Hongo, Bunkyo, Tokyo 113-8656, Japan
[2]Engineering Research Institute, The University of Tokyo, Yayoi, Bunkyo, Tokyo 113-8656, Japan

Introduction

We are now aiming at developing an optical system that can generate arbitrary X-ray polarization from horizontal linear X-ray polarization.

Perfect crystals show birefringence near the Bragg conditions and are used as X-ray phase retarders. The X-ray two-quadrant phase-retarder system we developed is composed of two transmission-type X-ray phase retarders and can compensate for off-axis aberration (phase-shift inhomogeneity due to angular divergence of incident X-rays)[1]. We also developed the X-ray four-quadrant phase-retarder system composed of four transmission-type X-ray phase retarders. The scattering planes of four phase-retarder diamond crystals are set to incline by 45°, 135°, 225°, and 315°, respectively, with respect to the direction of incident polarization. It can compensate for both off-axis and chromatic aberrations[2].

In our optical system, X-ray four-quadrant phase retarders are mounted on a χ-circle goniometer so that they can be rotated all together around the X-ray beam. Each phase retarder placed on tangential bar-type goniometers is rotatable around diameter of the χ-circle. The system occupies 27 cm in the beam path.

Here we report on generation of 45° oblique linear polarization by the use of the rotatable four-quadrant diamond phase-retarder system.

Experimental

Horizontal linear polarization was converted into 45° oblique linear polarization along two different paths on the Poincaré sphere shown in Fig 1 and the results were evaluated and compared by an X-ray polarimeter composed of a polarizer and an analyzer. Intensities of rocking curves were measured at intervals of 20° of analyzer angle and each measuring time was 100 sec.

Path 1: Incident horizontal polarization was converted into clockwise circular polarization in the first stage, and was then converted into 45° oblique linear polarization in the second stage. The above two conversions were made by two sets of two-quadrant phase retarders. One placed in the downstream is rotatable, while one in the upper-stream is not.

Path 2: Incident X-ray was converted into 45° oblique linear polarization by using a rotatable four-quadrant phase-retarder system with the χ-angle set to be 22.5°.

Results and Discussion

Fig. 2 shows the experimental results with the polarimeter. The degree and azimuth angle of polarization were 0.952 and 55.8°, respectively, in the case of path 1, whereas they are 0.973 and 47.3°, respectively, in the case of path 2.

The azimuth angle of polarization obtained along the path 1 was different by 10° from the targeted value. There are two possible reasons conceivable for the error. Firstly, the phase shift given by the upstream two-quadrant phase retarder was smaller than intended. Secondly, the rotation axis of the down-stream two-quadrant phase retarder was slightly misaligned.

In the case of path 2, approximately 45° oblique linear polarization was obtained. The degree of polarization was also higher in the case of path 2 than path 1. This may be due to 1) compensation for chromatic aberrations by the use of four-quadrant phase-retarder system as a single component and 2) shorter path length of conversion on the Poincaré sphere.

In this experiment, we could generate 45° oblique linear polarization from horizontal linear polarization by using the X-ray four-quadrant phase-retarder. We are going to increase the accuracy in converting the polarization, and to generate arbitrary polarization including elliptically polarized X-ray, and to apply the system to experiments in which a switching between arbitrary polarizations is required.

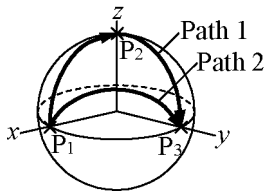

Figure 1
Polarization conversion paths on the Poincaré sphere. P_1: horizontal linear polarization. P_2: clockwise circular polarization. P_3: 45° oblique linear polarization.

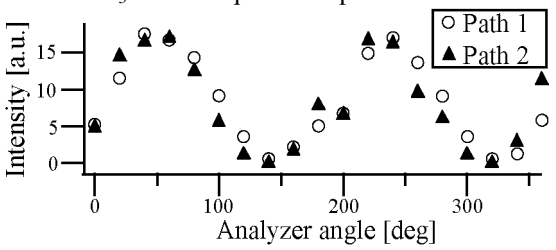

Figure 2
Intensities of rocking curves measured by the analyzer.

Reference

[1] K. Okitsu *et al*., J. Synchrotron Rad., **8**, 33 - 37 (2001).
[2] K. Okitsu *et al*., Acta Cryst., **A58**, 146 - 154 (2002).
* amemiya@k.u-tokyo.ac.jp

12A/2000G015

Absolute calibration of space-resolving soft X-ray spectrograph for plasma diagnostics

Masayuki YOSHIKAWA*[1], Takatoshi FURUKAWA[1], Keiichiro SEDO[1], Yuusuke KUBOTA[1], Takayuki KOBAYASHI[1] and Naohiro YAMAGUCHI[2]
[1]Plasma Research Center, University of Tsukuba, Tsukuba, Ibaraki 305-8755, Japan
[2]Toyota Technological Institute, Nagoya, Aichi 468-8511, Japan

Introduction

Measurements of spatial and temporal variation of spectra in the wavelength range from vacuum ultraviolet (VUV) to soft x-ray (SX) are necessary to determine radiation power losses and ion density profiles which directly relate to the impurity transport, confinement and sources in magnetically confined plasmas. We developed space- and time-resolving VUV (150-1050 Å) [1, 2] and SX (20-350 Å) [3, 4] spectrographs and applied for impurity diagnostics in the tandem mirror GAMMA 10.

For quantitative analyses of emission lines, it is important to characterize the absolute sensitivity of these spectrograph systems throughout their wavelength ranges. Previously we measured the absolute sensitivities of VUV spectrograph under incident polarized light conditions for wavelength range from 150 Å to 1050 Å [2]. In this report, we show the absolute sensitivity of the diffracting position on the concave grating in the SX spectrograph system (50-250 Å).

Experiments

In the space- and time-resolving SX spectrograph, a concave grating ruled with varied spacing (Hitachi P/N001-0266) is used, which has a nominal groove density of 1200 g/mm and a ruled area of 50 × 30 mm^2. The incident angle is 87 ° and the effective braze wavelength is 100 Å. The entrance slit is a 6-mm in height and 100 µm in width. A MCP intensified detector (Hamamatsu F2814-23P) having 50 × 50 mm^2 active area is set on the flat field output plane. The recording system of spectral image is a high-speed solid state camera (Reticon MC9256) with a fast scanning controller. The resolution of video image is eight bit. The frame rate with full image size, 256 × 256 pixels, can be changed from 4 to 106 frame/s.

The experiments have been carried out at the beam line 12A (BL-12A). The incidnet photon intensity was monitored just behind the entrance slit by using an absolutely calibrated XUV silicon photodiode (IRD AXUV-100G) and then the output spectral image was recorded by a high-speed camera. Measurements are repeated for wavelength range from 20 Å to 250 Å at the BL-12A with 20 Å intervals. We changed the incident light position on the grating at the three points, center (0mm), up (+3 mm) and down (–3mm).

Results

The absolute sensitivity of the SX spectrograph as a function of wavelength under the three diffracting positions on the grating for wavelength range from 50 Å to 250 Å is shown in Fig. 1. This shows that the SX spectrograph has not so clear sensitivity against the diffracting position on the grating. Then we plan to carry out the more experiments for sensitivity of diffracting efficiency against the incident angle of the SX spectrograph.

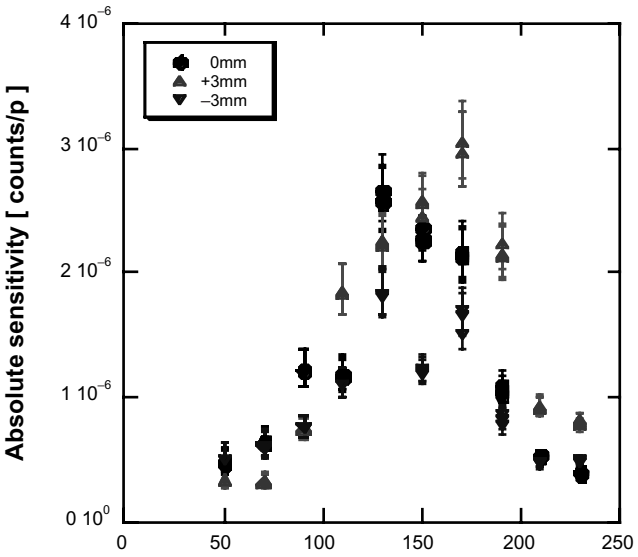

Fig. 1 Absolute sensitivity of the SX spectrograph.

References

[1] N. Yamaguchi et al., Rev. Sci. Instrum. **65**, 3408 (1994).
[2] M. Yoshikawa et al., Photon Factory Activity Report #18, 2001, Proposal No.2000G015.
[3] N. Yamaguchi et al., J. Plasma and Fusion Res. **71**, 867(1995).
[4] M. Yoshikawa et al., Nucl. Instrum. Methods Phys. Res. **A 467-468**, 1533 (2001).

* yosikawa@prc.tsukuba.ac.jp

14A/2000G022

Measurements by a silicon avalanche diode for observation of NEET on ^{193}Ir

Shunji KISHIMOTO*[1]
[1]KEK-PF, Tsukuba, Ibaraki 305-0801, Japan

Introduction

Nuclear excitation by electron transition (NEET) on ^{193}Ir in *K*-shell photoionization was observed with synchrotron radiation [1]. At BL-14A, measurements by a silicon avalanche diode and photodiodes were carried out to obtain parameters for NEET observation at SPring-8 and to calibrate the incident photon numbers for analysis of the NEET probability. The NEET on ^{193}Ir occurs between the $K(1S_{1/2}) : M_1(3S_{1/2})$ atomic hole transition (72.937keV) and the 73.041-keV nuclear transition (3/2+ : 1/2+, half life: 6.09ns). Compared with NEET on ^{197}Au, the energy difference between the atomic and nuclear transitions is larger, 104 eV and the nuclear matrix element is smaller than that of ^{197}Au. Thus, the NEET probability for ^{193}Ir is expected to be 2.3×10^{-9}, less than one tenth of that of ^{197}Au [2].

Experiments

The silicon avalanche diode (Si-AD, Hamamatsu SPL4583) was used to detect internal-conversion electrons emitted from excited nuclei. The device was 3 mm in diameter and had a depletion layer 30μm thick. The energy spectra of the avalanche diodes were investigated at BL-14A. An X-ray beam from a Si(553) double crystal monochromator was defined to $^{H}1.0\times^{V}1.0$ mm. We used an iridium target that was made of metal powder on aluminum foil. The Si-AD was installed in a vacuum chamber for the NEET experiment and was located 2.5mm above the target. A charge-sensitive preamplifier, Canberra 2001A, was used to investigate energy spectra while a fast amplifier, Philips Scientific 6954, was used for NEET experiments. In order directly to measure a pulse-height distribution of the fast amplifier's outputs, we took a single-channel scanning method with a constant fraction discriminator and a scaler.

The estimation of the incident photon number was also important to decide the NEET probability. Photodiodes (silicon PIN-PD, 500μm thick) were used to monitor intensity of the incident X-rays. The photon numbers per PD's current were obtained from results measured at BL-14A.

Results

Figure 1(a) shows an energy spectrum measured by the charge-sensitive preamplifier at an incident X-ray energy of 73.041keV. The main peak by *L*-photoelectrons and peaks of *L* X-rays at 9-11 keV are seen. Figure 1(b) shows a pulse-height distribution by the fast amplifier, measured at the same energy of the incident X-rays. The peak of *L*-photoelectrons was seen as a main profile. By comparing the peak position of *L*-photoelectrons, the threshold level of the discriminator, which was selected for the NEET experiments and was –20mV, corresponded to 32keV. One can see that the profile of *L*-photoelectrons measured at the nuclear excited level of 73.041keV approximated to the spectrum of the *L*-internal conversion electrons. Therefore, a signal which energy was larger than 32keV contributed to the time spectrum in the *L*-internal conversion electrons detected by the Si-AD.

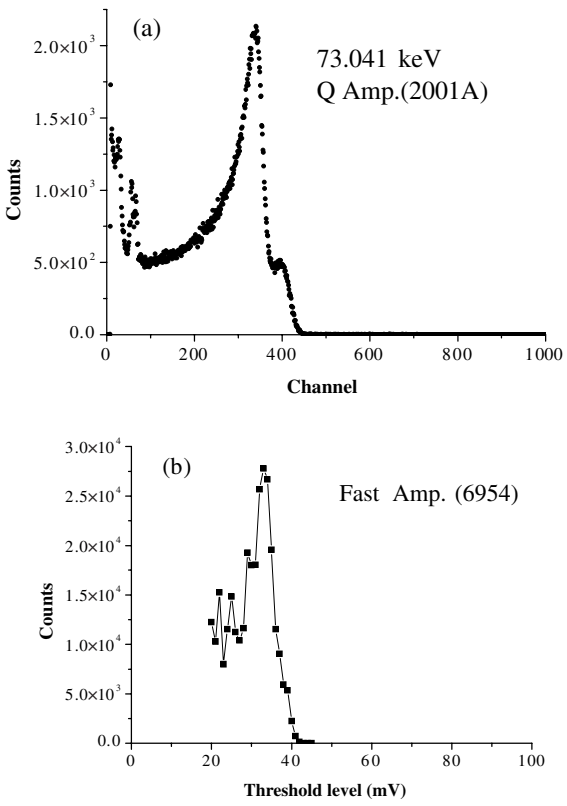

Fig. 1 Energy spectra of radiations emitted from the iridium target measured with (a) a charge-sensitive preamplifier and a normal spectroscopy system. Fig. 1(b) shows a profile measured with a fast amplifier by scanning threshold level of a discriminator. Energy of the incident X-rays was 73.041keV.

References

[1] S. Kishimoto et al., SPring-8 User Experiment Report No. 8 (2001B), p.67.
[2] E. V. Tkalya, private communications.

*syunji.kishimoto@kek.jp

14A/2000G041

A combination of accurate, synchrotron X-ray and quantitative electron diffraction for charge density measurement in α-Al_2O_3

Victor A. STRELTSOV*[1], Philip N. H. NAKASHIMA[1] and Andrew W. S. JOHNSON[2]
[1]Crystallography Centre,[2]Centre for Microscopy, University of Western Australia, Nedlands, 6907, Australia.

Introduction

Current X-ray diffraction techniques intended for "ideally imperfect" specimens provide structure factors only on a relative scale and ever-present multiple scattering (extinction) in strong low angle Bragg reflections is difficult to correct. Multiple dynamic scattering is implicit in the quantitative convergent beam electron diffraction (QCBED) method, which provides absolutely scaled structure factors. Conventional single crystal X-ray diffraction has proved adequate in softer materials where crystal perfection is limited. In hard materials, the highly perfect nature of the crystals is often a difficulty, due to the inadequacy of the conventional corrections for multiple scattering (extinction corrections). The present study exploits the complementarity of synchrotron X-ray measurements for weak and medium intensities and QCBED measurement of strong low-angle reflections for α-Al_2O_3.

Experimental

X-ray Diffraction. Synchrotron X-ray diffraction data set for α-Al_2O_3 was used to complement the QCBED data. This data consists of the X-ray diffraction intensities over complete sphere up to $(\sin\theta/\lambda)_{max}$=1.1 Å^{-1} measured at room temperature with λ = 0.7Å radiation using the BL14A beam line four-circle diffractometer. In order to reduce absorption and extinction effects, a tiny, naturally faced specimen with dimensions less than 50 μm was used. Analytical absorption, Lorentz and polarization corrections and anomalous dispersion were applied. Symmetrically equivalent reflections were averaged. Independent structural parameters, including the scale factor, positional and thermal displacement parameters for all atoms were refined by conventional full-matrix least squares including all observed 249 unique structure factors.

Electron Diffraction. Two dimensional, energy filtered zero order Laue zone CBED patterns from a variety of parallel sided and wedged α-Al_2O_3 platelets were recorded using a Philips 430 transmission electron microscope (TEM) with a Gatan Image Filter. A slit width of 10 eV was used to remove inelastically scattered electrons. The accelerating voltage was measured for each data set using deficiency lines due to higher order Laue zone (HOLZ) reflections visible in various zero zone disks. The variation of these measurements made at the same accelerating voltage settings was less than 0.2%. The recorded CBED patterns were firstly corrected for instrumental point spread function (PSF) using a new method developed by the authors. QCBED data have been matched using Bloch-wave and Multislice methods. The reproducibility of QCBED data is better than 0.5%.

Combined X-ray and QCBED data. The low angle strong QCBED structure factors were combined with middle and high-angle extinction-free data from synchrotron X-ray diffraction measurements. The multipole expansion model was refined with VALRAY [1] using the combined data. The refinement converged to R=1.16% with a total number of 249 structure factors and a total of 29 refined parameters.

Results and discussion

Static deformation charge density map ($\Delta\rho$) for α-Al_2O_3 in Fig. 1(*a*) was calculated after multipole refinement of the combined data and compared with density functional theory (DTF) calculation in Fig 1(*b*) based on WIEN2K [1] generalised gradient approximation (GGA) with the full potential linear augmented plane-wave method (FP-LAPW) [3]. The Fig. 1 maps are in excellent agreement. The overall topography of the static $\Delta\rho$ density is similar, and both maps have higher excess density peaks of ~0.28-0.32 e/Å^3 along the shortest Al-O1 bond (1.85Å) directions and a lower density of 0.24 e/Å^3 along the longer Al-O2 bond (1.97Å) directions.

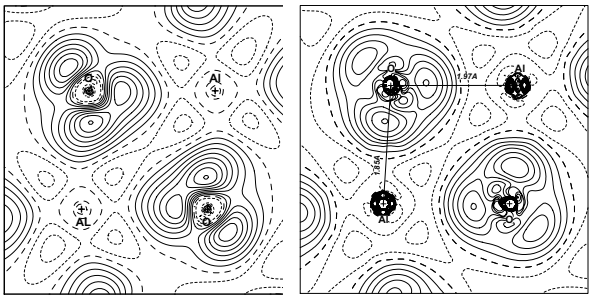

(*a*) (*b*)

Fig. 1. Static $\Delta\rho$ maps from (*a*) combined QCBED/XD data, and (*b*) *ab-initio* DFT calculations. The plane is through the Al and O – O common edge in α-Al_2O_3. Contour intervals are 0.04 e/Å^3 with solid lines positive and short dashed lines, negative.

The necessity for a complementary measurement technique producing absolute extinction free structure factors becomes evident. The reproducibility of QCBED measurements from independent data sets (different crystals, zone axes, beam tilts and accelerating voltages) and the resulting agreement with theoretical calculations inspires confidence in the whole methodology.

References

[1] R. F. Stewart et al., VALRAY98. (1998).
[2] P. Blaha, et al., WIEN2K (2001).
[3] V. A. Streltsov, P. Nakashima & A. W. S. Johnson, J. Microscopy and Microanalysis. In press. (2002).
*strel@crystal.uwa.edu.au

NE1A1/2000G197

Grazing incidence magnetic compton profile (GIMCP)

Hiroshi SAKURAI*[1], Fumitake ITOH[1], Hiromi OIKE[1], Katsuyoshi TAKANO[1], Xiaoxi LIU[2], and Hiroshi KAWATA[3]

[1]Dept. Electronic Eng. Gunma Univ., Kiryu, Gunma 376-8515, Japan
[2]SVBL Gunma Univ., Kiryu, Gunma 376-8515, Japan
[3]KEK-PF, Tsukuba, Ibaraki 305-0801, Japan

Nano-structured magnetic thin films, such as multilayers, show interesting properties. They come from modifications of wave functions at the interfaces. Magnetic Compton profiles (MCP) have been known as the probe of wave functions. However, it has been not easy to measure magnetic thin films because of strong background from a substrate. Recently, grazing incident X-rays (GIX) have been recognized as a good tool for thin films because the penetration depth is about a several hundred nm. Then, a magnetic Compton profile under the GIX (GIMCP) is expected to give information on the wave functions of the thin films with good signal-noise ratio. In this study we try to develop a system for measuring the GIMCP.

The incident monochromatized X-ray energy was 42.9keV. The scattering angle was 160 degrees. A beam size was 0.05 2mm^2. Cr buffer layer (20nm) and Fe layer (200nm) were sputtered on a polished glass (BK7) substrate (50ϕ×4t). The topmost was capped by C layer with 2nm. The Fe plate (10×30×0.1mm^3) was measured as a reference sample with an incident angle of 10 degrees. The measurement was carried out under the vacuum at R. T. The applied field on the sample was 0.5T. The background scattering from the window of vacuum chamber was about a several tens cps, which was less than 1% of total counts.

Figure 1 shows an experimental reflection curve of the sample. Critical angles of Fe-C interface: $\theta_{\text{Fe-C}}$= 0.065degree (the calculated value is 0.067 degree) is observed in Fig. 1.

Figure 2 shows energy spectra of scattered X-rays from the Fe 200nm on the substrate (a), the substrate (b) and the Fe 0.1mm(standard sample) (c). The spectra were adjusted to have the same Compton peak intensity. Because Ba K fluorescence (32.1keV) comes from the scattering at the substrate, the contribution of the substrate can be subtracted using the spectrum (b). Then the contribution from the Fe layer can be estimated to be 30% in the spectrum (a).

Figure 3 shows the GIMCP of the Fe 200nm. Solid line denotes the MCP of the standard Fe sample. The GIMCP reproduce the MCP of the standard Fe sample.

In conclusion we can succeed to develop a system for measuring the GIMCP. The GIMCP will become a good candidate, such XMCD, for measuring magnetic thin films.

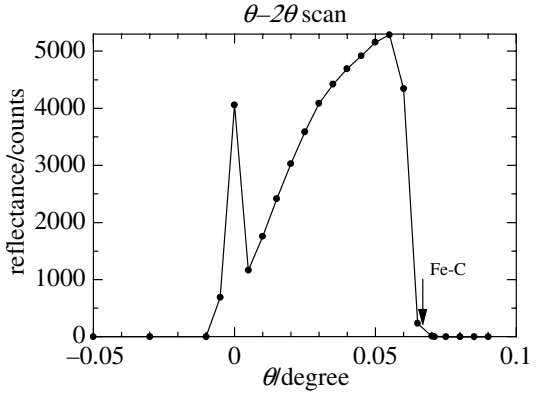

Fig. 1

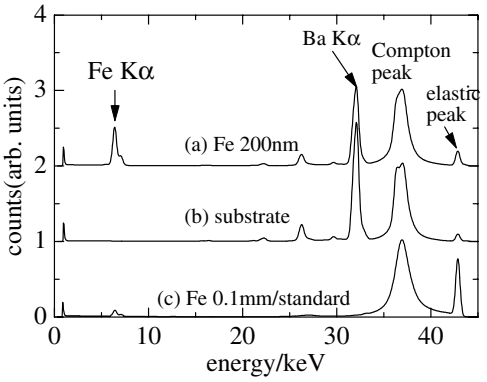

Fig. 2

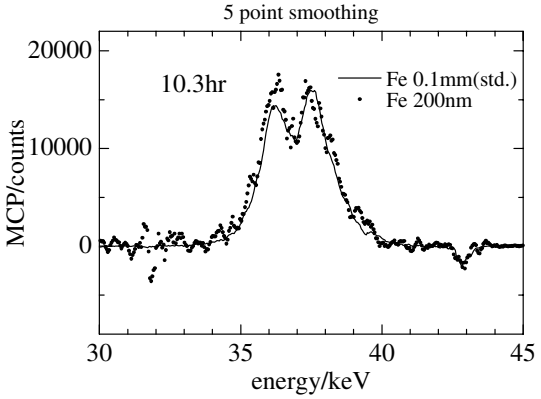

Fig. 3

*sakuraih@el.gunma-u.ac.jp

3C$_2$/2000G214

Phase-contrast hard X-ray microscope with a zone plate

H. Yokosuka[1], N. Watanabe[1], T. Ohigashi[1], S. Aoki[1], and M. Ando[2]
[1]Institute of Appl. Phys., University of Tsukuba, Tsukuba, Ibaraki 305-8577, Japan
[2]KEK-PF, Tsukuba, Ibaraki 305-0801, Japan

Introduction

In x-ray region, phase-contrast is much higher than absorption contrast especially for a specimen that consists of light elements, such as biological specimens. Phase-contrast imaging offers observation methods of a specimen that is almost transparent for X-rays. We have been developing a Zernike-type phase-contrast x-ray microscope with a zone plate and a phase plate [1] [2]. Recently, the resolution of the objective zone plate was improved. The present status of the microscope is reported.

Experimental

Figure 1 shows the optical system. X-rays from the bending magnet source were monochromatized with a Si (111) double crystal monochromator. Parallel monochromatic x-rays at 9keV were incident on a specimen. The x-ray image was focused on a detector by a zone plate. The specifications of the zone plate were the followings; (diameter: 155μm, the outermost zone width: 0.1μm, pattern thickness: Ta 1μm, substrate: SiN 2.2μm, focal length at 9keV: 113mm). The magnification ratio was about 19. A CCD camera (Hamamatsu C4880, CCD: Texas Instruments TC-215, pixel size: 12 μm) and nuclear emulsion plates (Fuji EM G-OC 15) were used as a detector.

A phase plate was placed at the back focal plane of the zone plate. Two types of phase plates were tested. One was an aluminum phase plate of 5μm thickness, the center of which was a 12μmϕ pinhole. The phase shift is calculated to be a quarter wavelength for scattering x-rays from a specimen. Figure 2(a) is a bright field image of polystyrene latex beads (diameter: 2.8μm) without the phase plate, and Fig.2(b) is a phase-contrast image with the phase plate.

Another phase plate was a gold wire of 10μm diameter embedded in epoxy resin (Quetol 651). The slice of 7 μm thickness was cut down and used as a phase plate. The phase shift and the transmittance of 7 μm-thick gold is 1.9 λ and 13 %, respectively. The phase shift of the epoxy resin is 0.16λ, which is estimated from Quetol 651 monomer. Then, non-scattering x-rays from a specimen are advanced by approximately one and three quarter wavelength in phase. Figure 3 shows images of a tantalum test pattern. The specifications of the test pattern were the followings; (pitch 0.1~ 0.4μm, pattern thickness: Ta 0.5μm, substrate: 2.0μm SiN). The images were recorded on nuclear emulsion plates and displayed as photographic negative. Figure 3(a) is the bright field image without the phase plate and Fig. 3(b) is the phase-contrast image with the phase plate. Much better contrast could be obtained in the phase-contrast image. The horizontal 0.1 μm line and space pattern could be observed in Fig. 2(b).

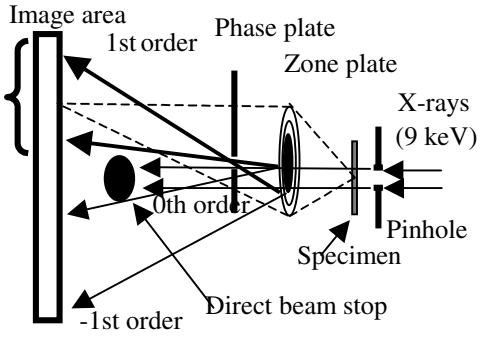

Figure 1: The optical system of the microscope.

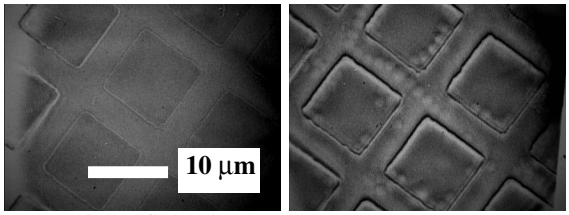

(a) Bright field image. Exposure: 360 s. (b) Phase-contrast image. Exposure: 360 s.

Figure 2: X-ray images of the polystyrene latex beads

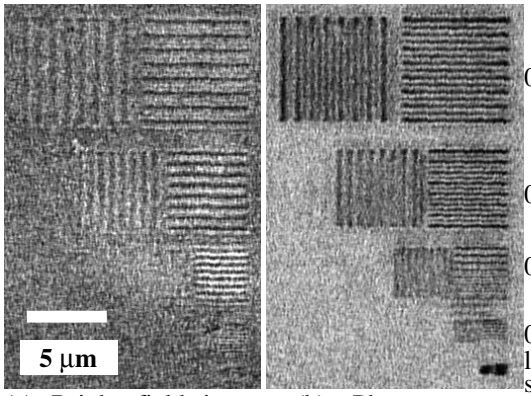

(a) Bright field image. Exposure: 60 s. (b) Phase-contrast image. Exposure: 240 s.

Figure 3: X-ray images of the tantalum test pattern

References

[1] PF Activity Report, #18. B. P.290
[2] H. Yokosuka, et al., J. Synchrotron Rad., **9** (2002) 179-181.

*yokosuka@aokilab.bk.tsukuba.ac.jp

16A1/2001G144

Commissioning of a multilayer monochromator for obtaining a high-flux beam from a multipole wiggler source

Kenji SAKURAI[1*], Mari MIZUSAWA[1] and Atsuo IIDA[2]
[1]National Institute for Materials Science, Tsukuba, Ibaraki 305-0047, Japan
[2]Photon Factory, Tsukuba, Ibaraki 305-0801, Japan

Introduction

A non-scanning XRF microscope [1] is a new procedure for the imaging of chemical composition. It uses quite a wide beam (12mm(H)×0.2mm(V)), which illuminates the whole sample surface in a grazing-incidence arrangement. The advantage is a short measuring time, typically around 1~2 min for one image (14 bit, 1M pixels) when using monochromatic X-rays at a bending magnet source. In order to consider more advanced experiments like real-time movies, a further strong photon flux is required. In the present research, a multiplayer monochromator has been designed as a multipole wiggler source.

Instrumentation

Fig 1 shows a photograph of a monochromator equipped with two multilayers (W/B_4C, 2d=50.36 Å, 125 layer pairs, 20mm×50mm×5mm, Osmic Co., Ltd.), both of which have independent stages for adjusting height and tilting. The other long translational stage ensures a constant height for the exit beam when changing X-ray energy. The 1st multilayer is cooled indirectly, i.e., supported by a water-cooled copper plate. The temperature is 22 ℃. The whole monochromator has been installed in a vacuum tank.

The experiment was carried out at BL-16A1. A single beamline-mirror (Rh coated, 4.5 mrad incidence) was used for rejecting high-energy X-rays. The present multilayer monochromator was placed in the experimental hutch (~35.5m from the source). A Si PIN detector (XR-100T, Amptek, energy resolution ~200 eV at 5.9 keV) was employed for measuring the X-ray energy of air scattering from an X-ray path. Ionization chambers are also used for monitoring intensity.

Results

Fig 2 shows typical spectra from air scattering. The energy band width is 578 eV at around 8 keV (~7%). The high-energy X-ray background is still visible, and therefore improving the signal to background ratio is necessary for XRF applications. In the present case, when 10 keV X-rays were used, the ratio improved notably and XRF imaging was achieved satisfactorily for the most part. Preliminary estimation indicates that flux intensity here is at least 100 times larger than that for a normal monochromatic beam at a bending magnet beamline. Some XRF movie experiments with the present monochromator are planned for the very near future. The authors wish to thank Drs. H. Sawa, Y. Wakabayashi and Y. Uchida for their assistance during the experiment.

References

[1] K.Sakurai, PF Activity Report #18, 279 (2000).
*sakurai@yuhgiri.nims.go.jp

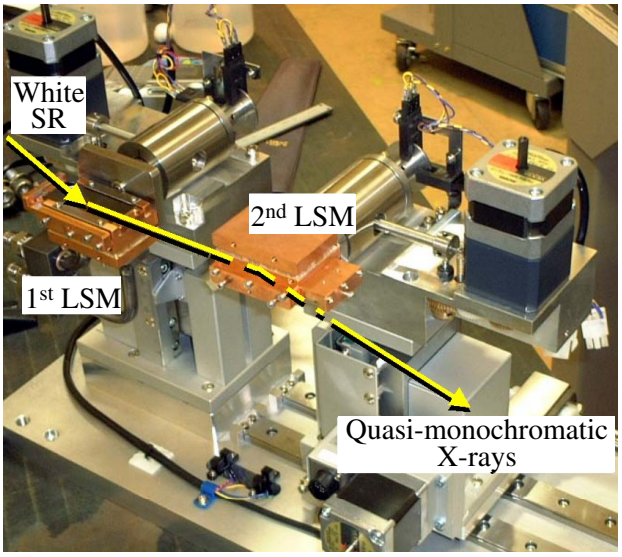

Figure 1 (up) A multilayer monochromator.
Figure 2 (right) Typical spectra for monochromatized X-rays. X-rays scattered by air were measured by an energy-dispersive detector.

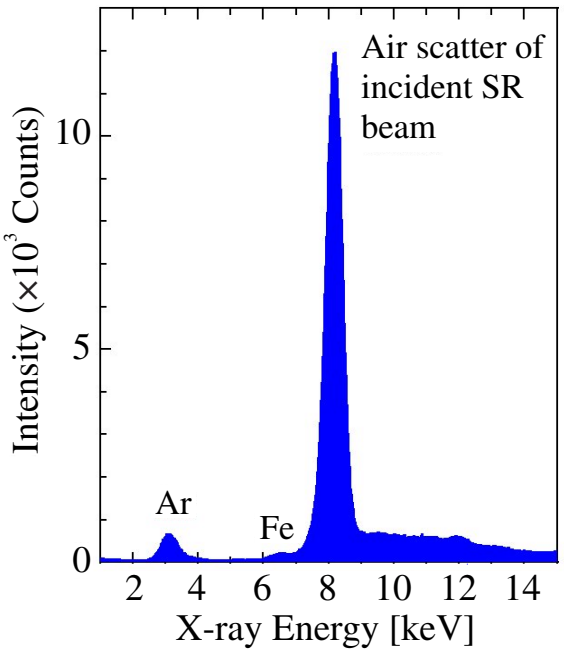

4A/2001G144

X-ray absorption fine structure imaging by a non-scanning X-ray fluorescence microscope

Kenji SAKURAI* and Mari MIZUSAWA
National Institute for Materials Science, Tsukuba, Ibaraki 305-0047, Japan

Introduction

X-ray absorption fine structure (XAFS) imaging using XRF intensity [1] is a very strong scientific tool because it provides spatial distribution on chemical composition as well as structural phases. Unfortunately, the imaging usually requires a fairly long measuring time, because the technique uses 2D scans. Our previous experience [2,3], however, indicates that non-scanning imaging can be a good alternative for quick observation. This report describes that this novel XRF microscope is suitable for recording XAFS imaging with 1 M pixels.

Experimental

The main idea of the present non-scanning XRF microscope has been described elsewhere [2]. A grazing-incidence arrangement is employed to make primary X-rays illuminate the whole sample surface. Parallel-beam optics and extreme-close-geometry (the clearance is ~0.5mm or less) are adopted in order to detect XRF from the sample. A CCD camera is mounted on the frame with a downward-looking arrangement like a usual optical microscope, while conventional scanning XRF imaging uses a sideways-looking arrangement, which means the sample is stood up and has a vertical rotation axis. The view area is 12mm(H)×12mm (V). The pixels are around 1000×1000. To perform XAFS imaging, the exposure has been repeated during scanning of the primary photon energy. The typical exposure time is 60 sec/point. XAFS spectra were obtained by integration of the XRF intensities in the interested pixels.

Results

Figure 1 shows typical Fe K XAFS spectra obtained from XRF intensity from a specific area (the dark part in the photograph) of the rock sample. One can confirm XAFS oscillation is successfully recorded, and in principle, detailed atomic-structure is available. Although the present case is quite simple, it is possible to perform structural imaging, even for rather complicated samples including different phases, e.g., amorphous and several different crystalline materials. Another feasible experiment is chemical state imaging based on the selective-excitation of specific chemical species by means of absorption edge shifts. The authors would like to thank Prof. A. Iida for his valuable assistance.

References

[1] K.Sakurai, A.Iida, M.Takahashi and Y.Gohshi, Jpn. J. Appl. Phys., **27,** L1768 (1988).
[2] K.Sakurai, Spectrochimica Acta B54, 1497 (1999).
[3] K.Sakurai, PF Activity Report #18, 279 (2000).
*sakurai@yuhgiri.nims.go.jp

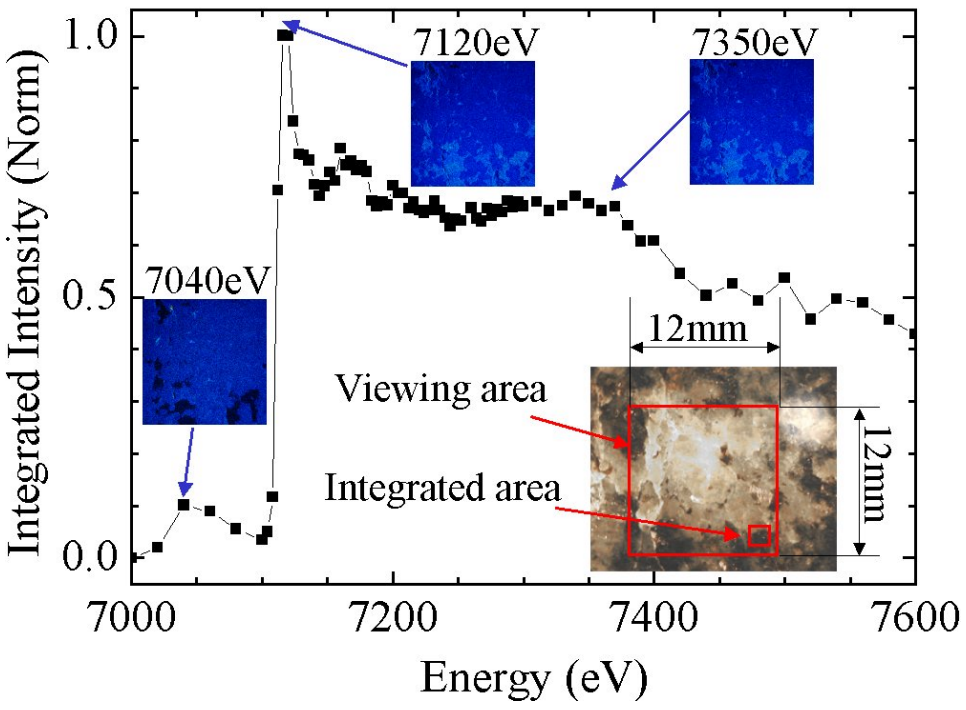

Figure 1

Example of XAFS imaging. The spectra are from a specific area (the dark part in the photograph) of the rock sample, Amphibole Gabbro, collected at the top of (Mt. Tsukuba. The set of image data includes such spectral information for each pixel. Measuring time, 60 sec for one point.

9A,12C/2001G319

Development of light-modulated XAFS spectroscopy (2)

Kaoru OKAMOTO[1], Kenji KOHDATE[1], Kensuke NAGAI[1], Jun MIYAWAKI[1], Hiroshi KONDOH[1], Toshihiko YOKOYAMA[2], Shuichi EMURA[3], and Toshiaki OHTA*[1]
[1] Department of Chemistry, School of Science, the University of Tokyo, Hongo, Bunkyo-ku, Tokyo 113-0033, Japan
[2] Institute for Molecular Science, Myodaiji-cho, Okazaki, Aichi 444-8585, Japan
[3] The Institute of Scientific and Industrial Research, Osaka University, Mihogaoka, Ibaraki, Osaka 567-0047, Japan

Structural and electronic changes upon photo-excitation have been studied by various methods. In the case of materials with no long-range ordering, XAFS is one of the most useful tools to obtain direct information on local structures and electronic properties. However, it is quite difficult to observe dynamic behaviours by the conventional XAFS method. The purpose of this study is to apply the light-modulation method, which is widely used for Raman, IR, and UV-vis spectroscopies, to x-ray absorption spectroscopy. Previously, we reported the detection of light-modulated XANES and EXAFS spectra using a Xe-arc lamp as the visible light source [1]. However, the possibility of heating effect upon light irradiation should be eliminated. Thus, we performed similar experiments using a low-power laser.

All measurements were carried out in the fluorescence mode at BL-9A and 12C with double-crystal Si(111) monochromators detuned by ~40%. The incident x-rays were detected by an ionization chamber filled with N_2 and fluorescent x-rays by a Lytle detector filled with Ar. Experimental setup is shown in our previous report. A focused Xe lamp (supplied power of 300 W, 350-700 nm) and a Nd-YAG laser (50 mW, 532 nm, spot diameter of 3~4 mm at the sample position) were used as the light sources. To avoid noises caused by the signal fluctuations after moving the monochromator, the signal counter was controlled by an external timer circuit and waited before counting for ~15 seconds. To avoid vibration, the Lytle detector was set on silicone rubber insulators. Acquisition time was 10 or 20 seconds for each data point. A light-induced spin-crossover complex $Fe(pic)_3Cl_2 \cdot C_2H_5OH$ (pic=2-aminomethylpyridine) (**1**) powders were dispersed on Scotch tapes and used as the sample. All spectra were normalized to the edge jumps, and outputs of the lock-in amplifier were corrected to the original order.

Figure 1 shows light-modulated Fe *K*-edge XANES difference spectra of **1** at various temperatures. Under laser irradiation the difference is largest at 49 K and smaller at higher temperatures (Fig.1(a)). It is natural because the lifetime of the trapped state decays upon warming. However, under Xe-lamp irradiation, the order depends on light intensity. At BL-9A, the difference is smaller at higher temperatures (Fig.1(b)), while it is larger at BL-12C (Fig.1(c)), where geometrical limitation does not allow to collect enough light from the light source. The light-induced spin-crossover transition of **1** shows a threshold behavior upon light intensity [2]. This could be the origin of the strange temperature dependence seen in Fig.1(c): under weak light irradiation **1** cannot be excited by light effectively and the contribution of local heating increases, while using intense light over the threshold light excitation becomes the main contributor. A low-power laser is ideal as the light source because such a problem will not arise.

[1] K. Okamoto et al., PF Activity Report 18, 293 (2001).
[2] Y. Ogawa et al., Phys. Rev. Lett. 84 (2000) 3181.

* ohta@chem.s.u-tokyo.ac.jp

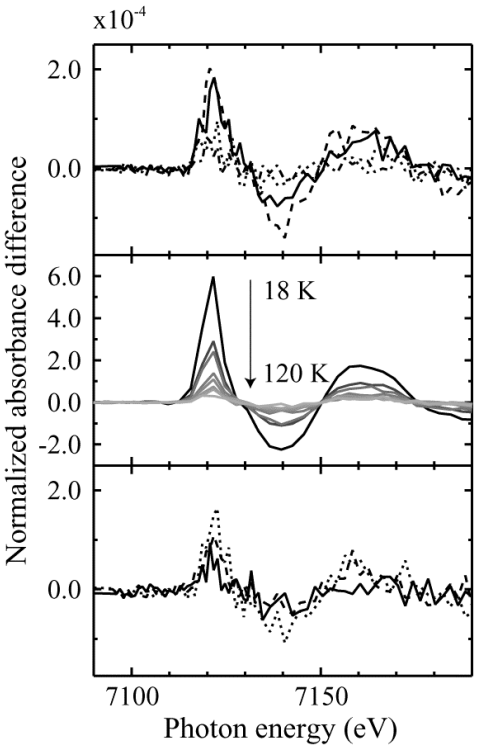

Fig. 1. Light-modulated Fe *K*-edge XANES difference spectra (a) under Nd-YAG laser irradiation at 30 K (solid line), 49 K (dashed line), 67 K (dotted line), and 96 K (dash-dotted line), (b) under intense Xe-lamp irradiation on warming process from 18 K to 120 K at BL-9A, and (c) under weak Xe-lamp irradiation at 29 K (solid line), 41 K (dashed line), and 61 K (dotted line) measured at BL-12C. The modulation frequency was 10 Hz for (a) and (c), and 5 Hz for (b). The differences on S/N ratios are mainly due to the difference of the amplifier risetime.

14C/2001G337

Response of GafChromic MD-55 film to synchrotron radiation

Nobuteru NARIYAMA*[1], Yoshihito NAMITO[2], Syuichi BAN[2]
[1]JASRI, Sayo, Hyogo 679-5198, Japan
[2]KEK, Tsukuba, Ibaraki 305-0801, Japan

Introduction

Recently, owing to the increase of synchrotron radiation facilities such as SPring-8, dose measurements of high-intense low-energy photons are increasingly needed for radiation protection and medical researches. For the dose measurement, tissue equivalence of dosimeter material becomes important.

A radiochromic film that has sensitivity in the dose region of several Gy to 100 Gy has been used in medical applications [1]. The film is thin and mainly composed of polyester. The purpose of this study is to measure responses of the double-layer GafChromic film for synchrotron radiation.

Materials and method

The experiment was carried out at BL-14C beamline. The exposure was monitored with a parallel plate free-air ionization chamber within 2.8% accuracy. The beam shape was collimated into a rectangle of about 10-mm long and 10-, 4- and 3-mm wide for 10, 30 and 40 keV photons, respectively. The doses of 2-150 Gy were given by changing the exposure time.

To be irradiated in free air, radiochromic films were set on the Scotch tape extended between acrylic poles and scanned horizontally during exposure to avoid beam strength inhomogeneity. The accuracy of the dose estimation depends not only on the accuracy of the ionization chamber but also on that of the readings of the beam cross-section length and the scanning speed. The former accuracy is considered to be 2-3% and the latter is below 1%.

The dosimeter film used was double-layer GafChromic MD-55 (ISP Technologies Inc.). The optical density was measured by 670-nm wavelength using FWT-100 radiachromic reader of Far West Technology two days later after the exposure.

The film sensitivity depends on the temperature and humidity during and after the exposure, which shows 5% fluctuation at most between 10 ℃ and 40 ℃ for 40 Gy [1]. The temperature in the experimental hutch was constant at 22 ℃, while the temperature at the ^{60}Co calibration was 10 ℃. In the case, the absorbance for synchrotron radiation possibly decreased by 3% owing to the temperature difference.

Results

Figure 1 shows the measured energy response of MD-55, which is normalized at ^{60}Co gamma rays: 0.592, 0.592, 0.581, 0.662 and 0.724 at 10, 15, 20, 30 and 40 keV. Chiu-Tsao et al have obtained 0.56 value for ^{125}I [2] and McLaughlin et al 0.63-0.66 at 20-40 keV and 0.61 at 15 keV [3]. Between 30 and 40 keV, the values appear to be smaller than those in Fig. 1, while the experiments of the other authors were made using broad energy spectrum source. The response of MD-55 having one active layer measured at BL-14C was also smaller at 30 keV, while the responses at 10 and 15 keV were larger than those in Fig. 1 [4].

The energy response was calculated using a photon-electron Monte Carlo transport code EGS4 [5]. The result is shown in Fig. 1, which is smaller than the measurements by about 10%. Considering the measurement errors of 4% for ^{60}Co calibration, 3% for reading of MD-55, 2% for the ionization chamber, 3% for the scanning method and 3% due to the temperature dependence, the discrepancy is considered to be within the errors.

References

[1] AAPM, AAPM Report No. 63 (1998).
[2] S. Chiu-Tsao et al., Med. Phys. **21**, 651 (1994).
[3] W.L. McLaughlin et al., Radiat. Prot. Dosim. **66**, 263 (1996).
[4] T. Kron et al., Phys. Med. Biol. **43**, 3235 (1998).
[5] W.R. Nelson et al., SLAC265 (1985).

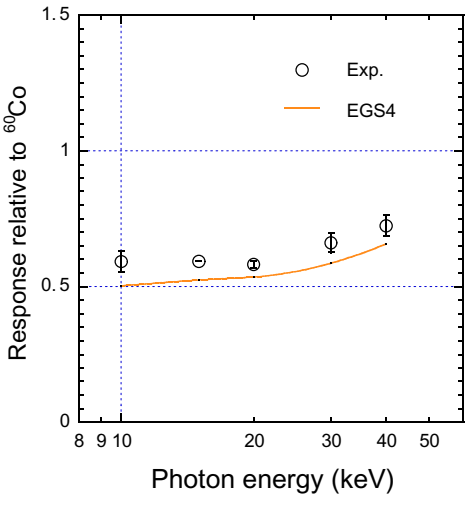

Fig. 1 Energy response of MD-55

* nariyama@spring8.or.jp

11A/2001P001

Soft X-ray transmission of an optical blocking filter for a X-ray CCD camera

Shunji KITAMOTO*[1], Takayoshi KOHMURA[1], Kazuharu SUGA[1], Eiji OZAWA[1], Kazuma SUZUKI[1], Risa KATOH[1], Yusuke TACHIBANA[1], Yusuke TSUJI[1], Ken KOGANEI[1], Kiyoshi HAYASHIDA[2], Haruyoshi KATAYAMA[2], Yusuke NAKASHIMA[2], Hideyuki ENOGUCHI[2]

[1] Department of Physics, Rikkyo University, 3-34-1, Nishi-Ikebukuro, Toshima-ku Tokyo, 171-8501,
[2]Department of Earth and Space Science, Osaka University, 1-1, Machikaneyama, Toyonaka, Osaka, 560-0043

Introduction

A Charge Coupled Device can be used as an X-ray Detector and has many wonderful advantages. As well as good imaging capability with less than 10μm, if it is used as a photon detector, it has almost ideal energy resolution of Si detector. Thus CCDs are now widely used as soft X-ray detectors.

We are planning to install CCD cameras on the Japanese 5th X-ray astronomical satellite, Astro-E2, which is now scheduled to launch in early 2005, Since a CCD has high detection efficiency for optical light and ultra violet light, we will use an optical blocking filter in front of the CCD chips. The experimental calibration of the soft X-ray transmission of them is very important. Especially the X-ray transmission properties around the absorption edges are comples[1] and must be determined by a measurement. We measured the soft X-ray transmission of an engineering model of the optical blocking filter.

The design parameter of the optical blocking filter is summarized in table 1. It is a polyimide sandwiched by aluminium (Al). The polyimide is mainly composed of carbon (C), and oxygen (O). Thus we focused on the measurement of the transmission around the K-absorption edges of Al, O, and C.

Measurement and Results

The BL - 11A line provides us good quality monochromatic soft X-rays between 90eV and 1900eV. This energy range covers the C-K, O-K and Al-K edges. When we measured the transmission around C-K and O-K edges, we used the second order rejection mirrors.

The beam was restricted by a slit. The sample optical blocking filter was installed on a rotational axle and it could be put in or be put off the beam. A window less photo diode (AXW-100 TS) was used as a detector and its current was measured. The windowless Si(Li) detector cooled by LN_2 was also used in order to check the energy spectrum of the beam.

The transmission of the optical blocking filter was calculated as a ratio of current with the filter and that without it. Derived transmission is shown in figure 1. The absorption fine structures around the absorption edges were clearly measured. The best-fit model transmission is also plotted in the same figures, where the absorption coefficients by Henke [2] are used and the materials are assumed to be composed of Al and polyimide. Although the discrepancy of the depth of O-K edge is prominent, the resultant thickness is listed in table 1.

Discussion

We measured the soft X-ray transmission of the optical blocking filter. The absorption fine structure was clearly obtained. The flight filters will be fabricated soon and we are now ready to calibrate the flight filters.

The discrepancy of the depth of the O-K edge means the existence of extra oxygen. One possibility is the oxidization of the aluminium. This possibility has been pointed out[3]. The oxidization of the aluminum might affect the optical transmission and actually unexpected transmission of the optical light is sometimes found. Thus the evaluation of the oxidization is very important.

We assumed the existence of a layer of Al_2O_3, adding to the original Al and polyimide layers and derived the best-fit thicknesses of them. The results are summarized in table 1. The next interest is the long-term change of the degree of the oxidization. This is our next subject.

Table 1: Thickness of the Materials

	Al	Polyimide	Al_2O_3
Design	1298Å	970Å	...
Simple Model	1151Å	1305Å	...
Oxidization Model	1006Å	1262Å	138Å

References

[1] Mori et al., NIM A, **A459**, 191-199(2001)
[2] B.L. Henke, E.M. Gullikson, and J.C. DavisAtomic Data and Nuclear Data Tables,**54**, 181-342 (1993).
[3] Kohmura. T.et al., Ad. Space. Res, **25**, 877-880 (2000).

*kitamoto@rikkyo.ne.jp

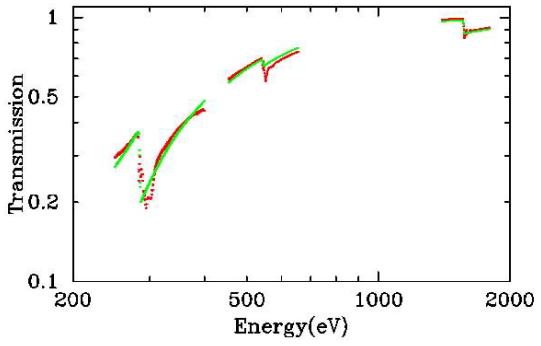

Fig.1 Measured transmission of the Optical Blocking Filter. The solid line is a model curve calculated using absorption coefficients by Henke et al. (1993).

3A/2001C001

A new system for *in situ* observation at liq./sol. interfaces

Masao KIMURA*[1] and Noriaki Ohta[2]
[1] Adv. Tech. Res. Lab., Nippon Steel Corp., Futtsu, Chiba, 293-8511, Japan
[2] Nippon Steel Technoresearch, Chiba 293-8500, Japan

Introduction

Electrochemical reactions are widely found in applicative as well as fundamental fields, such as corrosion, battery, catalysis and so on. One of its characteristics is that they occur at liquid/solid interfaces. *In situ* observation of reactions at the interface will give us a crucial information in order to understand the mechanism. In this study, a new system was developed for *in situ* observation of those reactions.

Design Concept

In order to perform *in situ* observation of electrochemical reactions at liquid/solid interfaces, the specimen under the film of water is investigated by x-ray scattering. The measured depth should be controlled easily in a range of nm-μm, because thickness of water and reaction-layer change as reactions progress. The electrochemical reactions is carried out in a special cell, where reaction parameters are controlled: the specimen potential, temp., pH, the gas potential inside the liquid., and so on.

The system was designed to satisfy the following conditions:

1) space for *in situ* cell
2) horizontal position of a specimen (the interface was easily retained during the reaction)
3) measuring both in- and out-of-plane scattering for surface-sensitive analysis
4) control of the angle of incidence of x-ray beam.

Results and Discussion

Based on the concept, a system ("EVA") was developed. The outline of the goniometer of the system was shown in Fig.1. A 2θ–θ goniometer ("χ-axis") was mounted on the table of another 2θ–θ goniometer ("θ-axis"). The combination of two diffractometer can be tilted against the x-ray beam form SR. The typical resolution of each axis is shown in Table1. Movement of each axis was controlled by PC through Ethernet.

Table 1 Resolution (deg.) of each axis

α : 2×10^{-5} ,	
χ2 : $<1 \times 10^{-3}$,	χ1 : $<8.4 \times 10^{-4}$
θ2 : $<1.4 \times 10^{-4}$,	θ1 : $<1.4 \times 10^{-4}$

This alignment enables to measure scattering intensities in a wide range of the reciprocal lattice, while controlling the incidence-angle (α_i) independently, which is called G-GIXS[1]. Two types of detector were used for measurement: an image plate (IP) and a NaI scintillation counter (SC) (Fig.2).

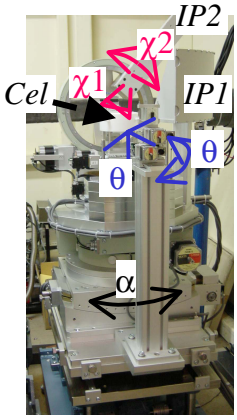

Fig.1 View of the goniomter of the EVA system

Then SC was used to scan the details of scattering intensities around Bragg peaks (Fig.2(b)). Two sets of slits, which limit the height and the width of the beam path, are positioned in front of the detector (Fig.2(b)). Resolution function was changed by altering the heights (h_{slit}), the width (w_{slit}), and the distance of two slits (d_{slit}=the distance S1-S2 in Fig.2(b)). The typical values are : h_{slit} w_{slit} and = 1-2 mm, d_{slit}= 310 mm; the resolution are $Q_{x\text{-}y} = 1\text{-}2 \times 10^{-2}$ and $Q_z = 2\text{-}4 \times 10^{-2}$ [r.l.u.].

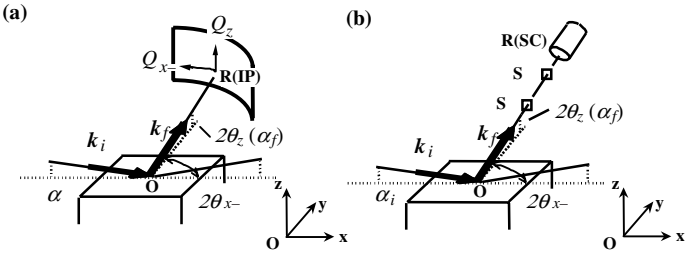

Fig.2 X-ray geometry for G-GIXS; (a) an image plate (IP) and (b) a NaI scintillation counter (SC) were used as a detector.

This system is now used for *in situ* observation of corrosion at metal surface with using a special cell at BL-3A at PF, KEK, Tsukuba, Japan.

We would like to thank Drs. T. Mori, M. Tanaka and T. Matsushita at PF for their great supports for experiments.

References

[1] Y. Takagi and M. Kimura: J. Synchrotron Rad., **5,** 488 (1998).

* kimura@re.nsc.co.jp